Endogenous desired debt in a Minskyan business model

Endogenous desired debt in a Minskyan business model

Lorenzo Cerboni Baiardi[a], Ahmad K. Naimzada[b], Anastasiia Panchuk[c]

[a] *Department of Economics and Management, University of Pisa, Italy*
[b] *Department of Economic, Quantitative Methods and Management Strategies, University of Milano-Bicocca, Italy*
[c] *Institute of Mathematics, NAS of Ukraine, Kyiv, Ukraine*

Abstract

We consider a Minskyan type model of a closed economy with autonomous public expenditure formulated in a discrete time framework, where an endogenous debt adjustment process is considered and where income variations account for real world physical and social constraints. The model is characterized by a unique nontrivial fixed point matching the economic equilibrium. We study its stability properties in terms of the constant factor that fixes the firms' desired debt level at a certain proportion of the current income. The stability loss of the fixed point is associated with either a subcritical flip or a supercritical Neimark-Sacker bifurcation. The latter implies occurrence of self-sustained oscillations interpreted as business cycles. We present three possible dynamic scenarios right after the Neimark-Sacker bifurcation: in a generic case and in two resonant cases. We also describe modifications of the attractor when propensity of firms to get into debt grows. In addition, we highlight that the increase of instabilities and complexities of dynamic outcomes is paired with the rise of the so called financial fragility indicator, which is a measure of fragility of the financial structure of the economy.

Keywords: Minsky hypothesis, financial fragility, business cycle, Neimark-Sacker bifurcation, critical lines.

1. Introduction

Minskyan type macroeconomic models are considered in [1] where the authors survey several mathematical formulations of the Minsky theory of economic crises based on the financial fragility concept, which explains how tranquil growth periods can be followed by speculative activities that lead to deep recessions and unstable economies (see [2–4]). This survey distinguishes the various models based on their focus on the key features characterizing the Minsky theory. In particular, we turn our attention to the circumstance where growing private debt to income ratio, describing firms' activities, increases the financial fragility and facilitates the emergence of economic instability.

Within this cluster and, in particular, in the stream of target debt-income ratio models, the contribution once presented at the 27th PKSG Annual Workshop[1] (see [5] and also the description in [1, p. 1319]) is placed. The authors consider a system in a continuous time framework, involving linear mechanisms for endogenous adjustments of income and debt levels. The debt alteration process is driven by the displacement of the current debt from the desired debt level, with the latter depending on the current economic scenario. In particular, in economic prosperity conditions, characterized by high income levels, the desired debt is high, thus reflecting low risk perceptions. Vice versa, in economic depression conditions, characterized by low income levels, the desired debt is low, thus reflecting high risk perceptions. In the model so formulated, the economic equilibrium is placed at the origin due to the lack of an autonomous component in the aggregate demand. Noteworthy, the authors showed that the debt to income proportionality coefficient has a destabilizing effect and that the fixed point can undergo a Hopf bifurcation beyond which limit cycles can be observed.

In the present work we reformulate the model proposed in [5] by making two methodological changes. First, we place our model in a discrete time frame-

[1] Held on June 1, 2017, at University of Greenwich.

work. This is suitable for future developments that include dependencies of income and debt adjustments to expectation formation and learning processes on incoming economic scenarios. Second, we introduce a nonlinear adjustment mechanism for income variations to adhere to real world circumstances. Indeed, material constraints in the production side of the economy as well as social bounds prevent unbounded growth variations.

Our map is characterized by a nontrivial fixed point, a circumstance occurring due to the introduction of an exogenous component in the aggregate demand given by the public expenditure. The stability properties of the fixed point are, as expected, affected by the proportionalty coefficient relating the desired debt level and the current income. Depending on the other parameter configurations, this constant factor can (i) have a destabilizing effect, (ii) can induce unconditional instability of the fixed point, or finally, (iii) have an ambiguous role, thus implying a double stability threshold. In particular, we shall see that, in the meaningful range of parameter values, the fixed point can lose stability either via a subcritical flip or via a supercritical Neimark-Sacker bifurcation. The latter leads to dynamics oscillating around the repelling focus and the map is capable of describe business cycle scenarios. It is also discovered that growing propensity of firms to get into debt can cause the rise of short term fluctuations that perturb the long term oscillatory behavior. We show that this occurs due to the intersection of the attracting invariant curve and the set of merging preimages. We further find out that if the desired proportion between debt and income is sufficiently high, an attractor is a chaotic area, which is confined by critical sets of different rank. Such complex behaviors are characterized by the persistence of high/low income and debt levels along extended time periods, which may be interpreted as chaotic business cycles. Finally, we consider the financial fragility indicator, defined as the ratio between the interest payments and the flow of profits, in terms of which the financial structure of the economy is characterized. In the framework of this model, we highlight the existing connection between increasing values of the financial fragility indicator and the increase of the dynamic instabilities and complexities.

The paper is organized as follows. In Section 2 the model is formulated and we show that debt and income variations are described by a two dimensional discrete time map. In Section 3 we prove the existence and uniqueness of the fixed point and we provide local asymptotic stability conditions. In Section 4, we perform a more detailed analysis of bifurcation structure of the parameter space. In particular, we provide three examples of the dynamics right after the Neimark-Sacker bifurcation: in generic case and in two resonant cases. In Section 5 numerical simulations are presented to outline the dynamic features of business cycles and the dynamic behavior of the financial fragility indicator is considered. Section 6 concludes.

2. A Minskyan type model

We consider a model of a closed economy with public intervention where the strictly positive government expenditure $\bar{G}$ is exogenously given and where the consumption C is increasing with the income Y. Investments I are entirely determined by both the income Y and the debt stock D in a way that will be expressed in an analytic form after the discussion on the firms' debt modeling. The aggregate demand Z is given by

$$Z = \bar{G} + C + I.$$

In the discrete time framework we consider, the consumption at period t results from the actual state of the economy, namely $C_t = cY_t$, where $c \in (0, 1)$ denotes the marginal propensity to consume. In addition, we assume that the investment level at time period t results from the current income and the debt levels and we set $I_t = I(Y_t, D_t)$. With this, the demand at time t is given by $Z_t = \bar{G} + C_t + I_t$.

The dynamics of the real economy is driven by the excess demand

$$E_t = Z_t - Y_t = \bar{G} + C_t + I_t - Y_t$$

by means of an adjustment mechanism according to which the income at time period $t + 1$ is given by

$$Y_{t+1} = Y_t + \alpha g(E_t), \tag{2.1}$$

where $\alpha > 0$ is a parameter that regulates the speed of adjustment. Recurrence (2.1) describes how the increase or decrease of the production depends on excess E_t. In particular, as usual in standard macroeconomic models, we require that an increase (decrease) of the income occurs at a positive (negative) demand excess. This is realized by requiring that the function $g : \mathbb{R} \to \mathbb{R}$ is increasing and with $g(0) = 0$. We stress that the origin corresponds to the macroeconomic equilibrium at which the demand excess vanishes, namely $Z_t = Y_t$. In Fig. 1 two examples of functional forms of g are provided. In order to adhere to real world

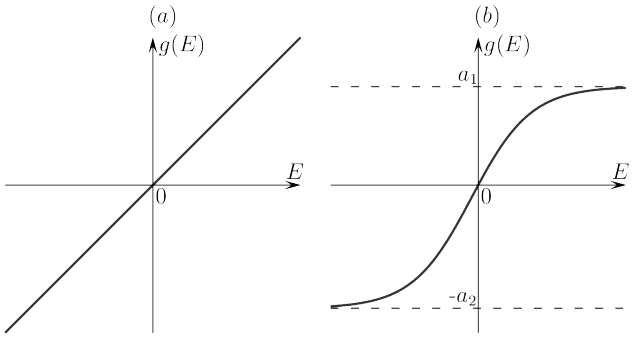

Figure 1: Function $g(E)$ of (a) linear and (b) sigmoid form.

circumstances, we avoid unbounded growth of income variations $Y_{t+1} - Y_t$ by introducing a saturation mechanism that accounts for the presence of material constraints in the production side of an economy. Indeed, when the demand excess increases, the capacity constraints will reasonably lead to lower increases in income, due to the limited expansion from time to time of capital and labor stock. On the other hand, when the demand excess decreases, capital cannot be destroyed proportionally as the only factors that may reduce productivity are attrition of machines from wear, time, and innovations. Motivated by the previous arguments, we consider that the adjustment mechanism of income is expressed through the sigmoid shaped continuous function g given by

$$g(E) = a_2 \left(\frac{a_1 + a_2}{a_1 e^{-E} + a_2} - 1 \right),$$

where a_1 and a_2 are positive parameters. As required, the sigmoid function g

is increasing and vanishing at the origin with slope

$$g'(0) = \frac{a_1 a_2}{a_1 + a_2}.$$

Moreover, the function g is bounded from below and from above by the horizontal asymptotes $-a_2$ and a_1 respectively, thus producing gradual changes of income variations. With this, the stepwise variation of income values cannot exceed the amplitude $2\alpha \max\{a_1, a_2\}$.

In the present model, we consider that at each period firms adjust their debt towards a certain desired level D_t^T determined by the constant factor $v > 0$ according to the relation $D_t^T = vY_t$. In such a modeling framework, the positive parameter v describes the aggregate action of firms, which are the more inclined to get into debt the higher the income level is. With this, we consider debt adjustments according to the following recurrence

$$D_{t+1} = D_t + \gamma(vY_t - D_t), \tag{2.2}$$

where the positive parameter γ regulates the speed of adjustment.

If we denote by ζ a fixed share of profits in total income, then total profits are equal to ζY. Without loss of generality we assume $c = 1 - \zeta$, that is the total consumption is equal to total wage income. By introducing the positive interest rate r, the debt use is expressed by the following equation

$$D_{t+1} - D_t = I_t - ((1 - c)Y_t - rD_t). \tag{2.3}$$

Such equation shows that the component of investments which is not financed by earnings must be financed by issuing new debt. The explicit expression of the investments is obtained plugging together equations (2.2) and (2.3) for debt variations, which leads to the following equation

$$I_t := I(Y_t, D_t) = \gamma(vY_t - D_t) + (1 - c)Y_t - rD_t. \tag{2.4}$$

The previous relation highlights that, as expected, investments are increasing with income and, at the same time, high debt levels discourages firms to invest.

Time variations of income and debt levels are provided respectively by recurrence (2.1) combined with (2.4) and by recurrence (2.2). This defines the two dimensional discrete time map T such that $T : (Y_t, D_t) \mapsto T(Y_t, D_t) := (Y_{t+1}, D_{t+1})$ where

$$\begin{aligned} Y_{t+1} &= T_1(Y_t, D_t) = Y_t + \alpha a_2 \left(\frac{a_1 + a_2}{a_1 e^{-(\gamma(vY_t - D_t) + \bar{G} - rD_t)} + a_2} - 1 \right), \\ D_{t+1} &= T_2(Y_t, D_t) = D_t + \gamma(vY_t - D_t). \end{aligned} \tag{2.5}$$

Remark 1. We mention that the quadrant $\mathbb{R}^2_+ := [0, +\infty) \times [0, +\infty)$ is not invariant under map T. This implies that certain componentwise positive initial conditions may be iterated outside the region $\mathbb{R}^2_+$, thus having no economic significance. In order to preserve the model capability of representing meaningful economic scenarios, we will limit our analysis to those orbits along which income, debt and investments maintain positive values.

Following the Minsky theory, we focus on the characterization of the financial structures of the economy in terms of the capability of firms to pay their debts. This concept is understood in terms of the so called financial fragility indicator f_t, defined as the ratio between the amount of interest payments rD_t and the flow of profits Π_t, that is

$$f_t := \frac{rD_t}{\Pi_t}.$$

Whenever the ratio f_t assumes values lower than the unity, the expected cash flows are sufficient to cover the existing financial obligations for period t, firms are financed at low risk. This is the case of hedge finance. Instead, when f_t assumes approximately unitary values, physical assets are financed at high risk, being the portion of cash flows owed to cover the payment of interests just sufficient to cover the payment of interests and the reimbursement of principal debt require new borrowing by firms. This is the case of speculative finance. The extreme occurrence where the financial fragility indicator exceeds unitary values represents high risky method of external financing, being profits not sufficient to cover even the interest due on outstanding debt. This is the case of ultra-speculative or Ponzi finance.

In the present model, where profits can be expressed as $\Pi_t = (1-c)Y_t$, the financial fragility indicator f_t can be rewritten as

$$f_t = \frac{rD_t}{(1-c)Y_t}. \tag{2.6}$$

3. Local bifurcation analysis of the fixed point

In this Section we provide the local analysis of the discrete time model. The existence and uniqueness of the fixed point of map T are stated in the following proposition.

Proposition 1. The unique componentwise positive equilibrium of map T is given by

$$F^* = (Y^*, D^*) = \frac{\bar{G}}{r}\left(\frac{1}{v}, 1\right). \tag{3.1}$$

Proof. It basically follows by imposing the stationary conditions $Y_{t+1} = Y_t$ and $D_{t+1} = D_t$. □

The level of income at fixed point F^* is, as expected, increasing with the public expenditure $\bar{G}$ while it is inversely proportional with respect to the factor v. Similarly, the debt equilibrium level is increasing with the public expenditure $\bar{G}$. Differently from the equilibrium configuration of the model formulated in [5], where both income and debt vanish, the fixed point F^* is characterized by strictly positive income and debt, a circumstance that follows from the aggregate demand including an autonomous component. Noteworthy, the fixed point F^* has an economic significance whenever it describes positive investments. Since at F^* investment are given by

$$I^* := I(Y^*, D^*) = \bar{G}\left(\frac{1-c}{rv} - 1\right),$$

it holds $I^* > 0$ whenever

$$v < \frac{1-c}{r}.$$

Moreover, the financial fragility (2.6) computed at F^* is given by

$$f^* := \frac{rD^*}{(1-c)Y^*} = \frac{rv}{1-c}. \tag{3.2}$$

This shows that, at equilibrium, the state of the financial structure of the economy depends on both the factor v and the interest rate r through a linear relation.

The following proposition highlights stability properties of F^* in terms of the parameter v.

Proposition 2. The fixed point F^* is locally asymptotically stable provided that

$$v_f < v \text{ and } v < v_{ns},$$

where

$$v_f := \frac{2\gamma - 4}{\alpha\gamma(2+r)} \frac{a_1 + a_2}{a_1 a_2}, \quad v_{ns} := \frac{1}{\alpha(1+r)} \frac{a_1 + a_2}{a_1 a_2}.$$

At $v = v_f$, F^* undergoes flip bifurcation while, at $v = v_{ns}$, it undergoes Neimark-Sacker bifurcation.

Proof. The trace and the determinant of the Jacobian matrix J^* of map T computed at fixed point F^* are given respectively by

$$\mathrm{tr}J^* = 2 - \gamma + \alpha\gamma v \frac{a_1 a_2}{a_1 + a_2}, \quad \det J^* = 1 - \gamma + \alpha\gamma v(1+r) \frac{a_1 a_2}{a_1 + a_2}.$$

The characteristic polynomial $p(\lambda)$ of the Jacobian J^*, defined as $p(\lambda) = \lambda^2 - \mathrm{tr}J^* + \det J^*$, computed at $\lambda = \pm 1$ gives

$$P(1) = \alpha\gamma r v \frac{a_1 + a_2}{a_1 a_2}, \quad P(-1) = 4 - 2\gamma + \alpha\gamma v(2+r) \frac{a_1 a_2}{a_1 + a_2}.$$

Jury's conditions for the asymptotic stability of F^* read as

$$\begin{aligned} &P(1) > 0 \text{ always satisfied,} \\ &P(-1) > 0 \text{ iff } v > v_f := \frac{2\gamma - 4}{\alpha\gamma(2+r)} \frac{a_1 + a_2}{a_1 a_2}, \\ &\det J^* < 1 \text{ iff } v < v_{ns} := \frac{1}{\alpha(1+r)} \frac{a_1 + a_2}{a_1 a_2} \end{aligned}$$

and the thesis follows. □

Proposition 2 marks an important difference between the model here formulated and that provided in [5] where the factor v has just destabilizing effects.

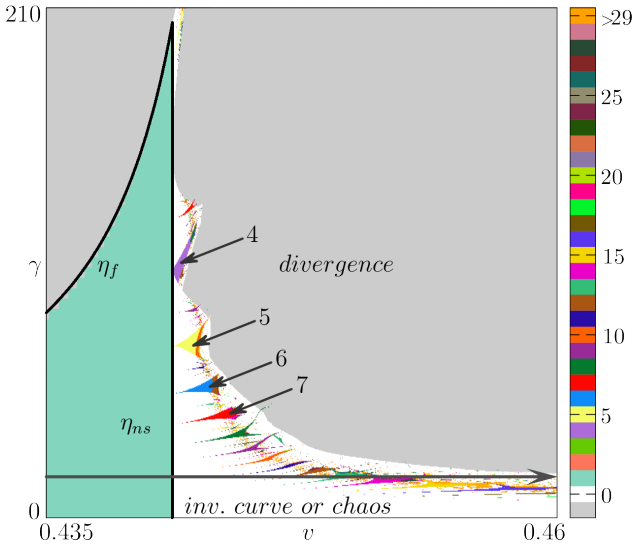

Figure 2: (Color online) Bifurcation structure of the (v, γ) parameter plane of T. Distinct colors correspond to different periods of cycles. Areas shown gray are related to divergent dynamics. The other parameters are $\alpha = 1, a_1 = 4, a_2 = 5, \bar{G} = 10, r = 0.02$. The horizontal arrow corresponds to $\gamma = 17$.

Differently, for map T the nonlinear saturation effects on income variations give to the parameter v an ambiguous role in determining the stability of the fixed point and a double stability threshold may be present.

Fig. 2 presents a 2-dimensional bifurcation diagram in (v, γ)-parameter plane, where bifurcation curves related to both flip, η_f, and Neimark-Sacker, η_{ns}, bifurcations are shown by solid lines. In particular, we identify three regimes where variations of v have different dynamic consequences. The first regime is characterized by the impossibility for the flip bifurcation to occur, being $v_f < 0$, which is possible provided that $\gamma < 2$. In this case, the parameter v has a destabilizing role and the fixed point F^* loses its stability through the Neimark-Sacker bifurcation whenever v is increased beyond the threshold v_{ns}. The second regime is characterized by the presence of a double stability threshold, that is, both the flip and the Neimark-Sacker bifurcations can occur, being $0 < v_f < v_{ns}$, which is possible provided that $2 < \gamma < 4(1/r + 1)$. In this second regime, an increase

of v from below to above the threshold v_f determines the stability retrieval of F^* via the flip bifurcation and a further increase of it beyond the threshold v_{ns} causes the stability loss of F^* via the Neimark-Sacker bifurcation. The third regime is characterized by unconditional instability of F^* due to nonexisting v satisfying both the stability conditions, being $v_{ns} \leq v_f$, which is the case if $4(1/r + 1) \leq \gamma$.

The Fig. 3 shows bifurcation diagrams of income (a), debt (b) and investments (c) varying the ratio v with other parameters kept fixed, which corresponds to the horizontal arrow shown in Fig. 2. We note that, along the mentioned bifurcation path, dynamic variables as well as investments maintain positive values. The represented dynamical scenario is placed in the second regime where both flip and Neimark-Sacker bifurcations can occur. However, we choose the range of v's that are mostly related to nontrivial dynamics. As follows from expressions of equilibrium levels Y^*, D^* and I^* (and confirmed by the plot in Fig. 3), when F^* is stable both income and investments decrease at increasing values of v while the debt is not affected. Then, when v exceeds the threshold v_{ns}, the fixed point F^* undergoes Neimark-Sacker bifurcation and orbits are attracted to the newly born invariant curve surrounding F^*. We also

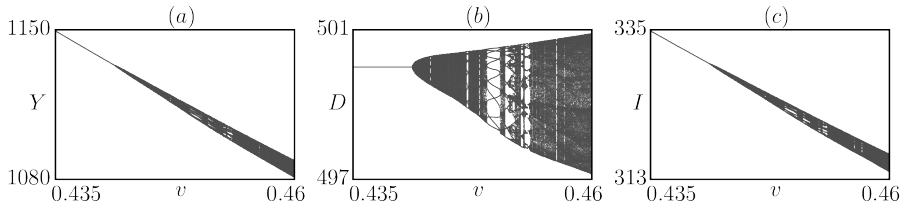

Figure 3: One-dimensional bifurcation diagrams versus v of (a) income Y, (b) debt D and (c) investments I for the same parameter set as in Fig. 2. The adjustment speed $\gamma = 17$ (the respective parameter path is shown in Fig. 2 by the black arrow) and the marginal propensity is $c = 0.7$.

remark here the existing connections between the local stability properties of the fixed point F^* and the fragility of the financial structure of the economy. To this purpose, we exploit relation (3.2), that expresses the value f^* of the

fragility at F^* as a linear function of the constant factor v. From this, it follows that an increase of v implies an increase of f^* that is further accompanied by the dynamic stability loss of F^* whenever v crosses the threshold value v_{ns}, at which the Neimark-Sacker bifurcation occurs.

4. More detailed analysis of flip and Neimark-Sacker bifurcations

In this section we provide a more detailed analysis of the map dynamics occurring after stability loss of the fixed point, as the parameter v crosses the flip or the Neimark-Sacker bifurcation value (for exhaustive description of these bifurcations the reader may refer to classical texts, for instance, [6–8]). In Fig. 2, one can see that for values $v < v_f$ the map exhibits only divergent orbits. As for the Neimark-Sacker bifurcation value η_{ns}, one observes the typical famous structure consisting of multiple regions related to attracting cycles of different periods emerging from η_{ns} (see, for instance, [9–11] to cite a few). Such regions are often called *Arnold tongues* or *mode-locking tongues*. They may also be observed in a certain class of circle maps and in 1D discontinuous piecewise increasing maps [12–14].

As already mentioned, when F^* loses stability through flip bifurcation at $v = v_f$ (with decreasing v), we observe no stable dynamics emerging. It means that for the chosen parameter set the flip bifurcation is subcritical. To understand whether it is always the case we need to construct the so called normal form for $v = v_f$. To simplify computation, we can get rid of the parameter $\bar{G}$, which influences only scaling of the variables Y and D. Indeed, the map T is topologically conjugate to the map $\widetilde{T} = \widetilde{T}_v : (Y_t, D_t) \mapsto (Y_{t+1}, D_{t+1})$ with

$$\begin{aligned} Y_{t+1} &= Y_t + \alpha a_2 \left(\frac{a_1 + a_2}{a_1 e^{-\gamma v Y_t + (\gamma + r) D_t} + a_2} - 1 \right), \\ D_{t+1} &= \gamma v Y_t + (1 - \gamma) D_t \end{aligned} \tag{4.1}$$

through the homeomorphism $h(Y, D) = (Y - Y^*, D - D^*)$. The map $\widetilde{T}$ has a unique fixed point $(0, 0)$, which undergoes a flip bifurcation at $v = v_f$.

Proposition 3. If $2 < \gamma < 4(1/r + 1)$, then there exists a neighborhood $U(v_f)$ such that for any $v \in U(v_f)$ map $\widetilde{T}$ given in (4.1) has a local one-dimensional invariant manifold W_v such that W_{v_f} is the central manifold at the moment of bifurcation. The restriction of map $\widetilde{T} = \widetilde{T}_{v_f}$ to its center manifold W_{v_f} is locally topologically conjugate near the fixed point $(0, 0)$ to the normal form

$$\eta \to -\eta + c(0)\eta^3 + O(\eta^4), \tag{4.2}$$

where

$$c(0) = \frac{2(\gamma - 2)(r + 2)^3(a_1^2 + a_2^2 - a_1 a_2)}{3(a_1 + a_2)^2(r\gamma - 4r - 4)}. \tag{4.3}$$

Proof. Proof is presented in Appendix A. □

The immediate implication from Proposition 3 is the following: provided that $2 < \gamma < 4(1/r + 1)$, the flip bifurcation, which the fixed point F^* of the initial map T undergoes at $v = v_f$, is *subcritical*. Indeed, all the terms (4.3) except for $(\gamma - 2)$ and $(r\gamma - 4r - 4)$ are always positive (given that all the parameters are positive). Hence, for the mentioned range of γ the coefficient $c(0)$ is negative. It guarantees that for $v > v_f$, which are at least sufficiently close to the bifurcation value, along with the stable fixed point F^*, there also exists a saddle 2-cycle $\mathcal{C}_2$, whose stable set confines the basin of attraction of the fixed point (see Fig. 4). At $v = v_f$ the cycle $\mathcal{C}_2$ collides with F^* and disappears. Then for $v < v_f$ the point F^* becomes a saddle and almost all orbits diverge.

Note that if $\gamma < 2$, then the flip bifurcation type changes to supercritical, but the value v_f becomes then negative (as has been already mentioned in the previous section), which is meaningless from the economic viewpoint.

Now we turn to deeper investigation of Neimark-Sacker bifurcation, whose main properties are described by

Proposition 4. If

C1. $\gamma \neq k(1/r + 1)$, $k = 2, 3, 4$,

then map $\widetilde{T}$, for values of v sufficiently close to v_{ns}, is locally topologically conjugate near the fixed point $(0, 0)$ to the normal form

$$z \to r(v)\mathrm{e}^{i\theta(v)}z + c(v)z|z|^2 + O(|z|^4), \tag{4.4}$$

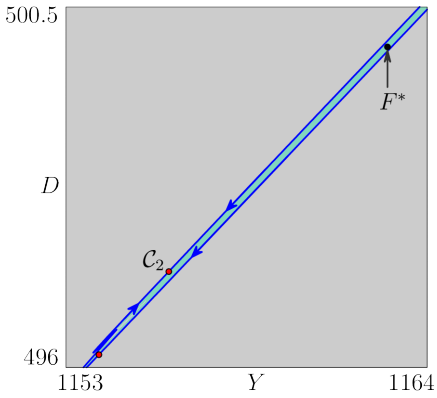

Figure 4: (Color online) Phase space of the map T with $\gamma = 17$, $v = 0.43$. Basin of attraction of the fixed point F^* is shown light-blue and is confined by the stable set (shown by blue arrows) of the saddle 2-cycle $\mathcal{C}_2$ (red points). Gray region is related to divergent orbits. The other parameters are as in Fig. 2.

where $z \in \mathbb{C}$, $c(v) \in \mathbb{C}$ and $r(v_{ns}) = 1$. Moreover, there holds

$$\Re\left(\mathrm{e}^{-i\theta(v_{ns})}c(v_{ns})\right) = -\frac{r\gamma^2((a_1-a_2)^2\gamma + 2a_1a_2)}{4(1+r)\alpha^2 a_1^2 a_2^2}. \tag{4.5}$$

Proof. Proof is presented in Appendix B. □

Since all parameters of the map T are positive, the expression in (4.5) is always negative. It means that when v increases over the threshold $v = v_{ns}$, regardless the other parameter values, the fixed point $(0, 0)$ of map $\widetilde{T}$, as well as the fixed point F^* of the initial map T, loses stability through the *supercritical* Neimark-Sacker bifurcation. Recall that, such a stability loss is related to the appearance of an attracting closed invariant curve surrounding the unstable fixed point F^*. In the applied context this is associated with occurrence of a business cycle, for which the economic interpretation is given in Sec. 5.

The structure of orbits right after the bifurcation differs depending on the parameters. Namely, the orbits can either be everywhere dense on the invariant curve or be attracted to a stable node cycle $\mathcal{C}_n^I$ of period n, which exists together with a saddle cycle $\mathcal{C}_n^{II}$ of the same period. The unstable set $W^u\left(\mathcal{C}_n^{II}\right)$ composes then the invariant curve. Generically, in the space of parameters there exist an

infinite number of regions $\mathcal{P}_n$ (Arnold tongues) associated with cycle pairs $\mathcal{C}_n^I$, $\mathcal{C}_n^{II}$. For parameter values being close to the Neimark-Sacker bifurcation curve, the boundaries of $\mathcal{P}_n$ are related to fold bifurcations at which the two respective cycles appear/disappear. In Fig. 2, one can clearly distinguish a sequence of tongues $\mathcal{P}_n$, $n \geq 4$, corresponding to so called *basic cycles*. With decreasing γ the period n increases and the regions $\mathcal{P}_n$ extend to larger values of v.

Let us consider as an example a generic tongue $\mathcal{P}_5$ related to a 5-cycle shown in Fig. 5(a). The upper and lower boundaries, $\eta_5^{fd,1}$ and $\eta_5^{fd,2}$, are related to fold bifurcations at which a stable node $\mathcal{C}_5^I$ and a saddle $\mathcal{C}_5^{II}$ appear/disappear, while at the third boundary η_5^{fl} the stable node cycle $\mathcal{C}_5^I$ undergoes a supercritical flip bifurcation leading to an attracting 10-cycle.

For parameter pairs located inside $\mathcal{P}_5$ sufficiently close to the Neimark-Sacker bifurcation curve, in the phase space of the map T there exists an invariant curve Γ composed by the unstable set $W^u\left(\mathcal{C}_5^{II}\right)$ of the saddle $\mathcal{C}_5^{II}$, all branches of which end up at points of the stable $\mathcal{C}_5^I$. In Fig. 5(b) we present an area of the phase space of T with $\gamma = 70.7$, $v = 0.4413$ containing the cycles $\mathcal{C}_5^I$ (blue points) and $\mathcal{C}_5^{II}$ (red points) together with the invariant curve Γ (red line). The parallelepiped area (which is outlined black in Fig. 5(b)) with vertices $(1132.92, 499.959)$, $(1133.08, 500.033)$, $(1133.095, 500.033)$ and $(1132.935, 499.959)$ is shown scaled in Fig. 5(c). The basin of attraction of $\mathcal{C}_5^I$ is confined by the stable set of some saddle cycle, whose exploration is beyond the scopes of the current paper.

With increasing further the value of v, a sequence of flip bifurcations associated with the cycle $\mathcal{C}_5^I$ occurs, due to which narrow regions related to cycles of period $5 \cdot 2^k$, $k \geq 1$, may appear. At a certain moment a $5 \cdot 2^k$-piece chaotic attractor is observed, whose pieces then merge pairwise with increasing v. At a certain "critical" value of v, this chaotic attractor is destroyed due to the boundary crisis, that is it collides with the boundary of its basin of attraction and for larger v almost all orbits diverge.

We remark here that even if the phenomena related to the periodicity tongue associated with period 5, described above, occur when the value of adjustment

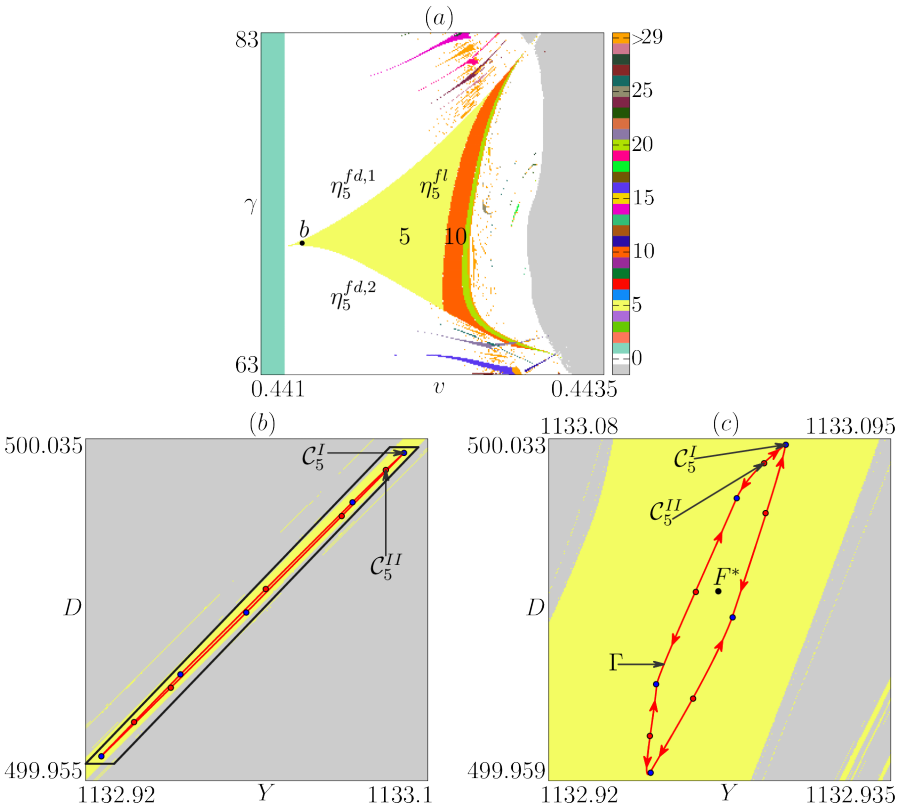

Figure 5: (Color online) (a) Periodicity region $\mathcal{P}_5$ related to period 5 in the (v, γ) parameter plane. (b) Phase space for the point marked 'b' in (a) with $\gamma = 70.7$, $v = 0.4413$. (c) Scaled parallelepiped area (with vertices $(1132.92, 499.959)$, $(1133.08, 500.033)$, $(1133.095, 500.033)$, $(1132.935, 499.959)$), which is outlined black in (b). Other parameters are as before.

speed γ is large, this value is still relatively small with respect to the values of income, Y_t, and debt, D_t. Also the term $\gamma(vY_t - D_t)$ in the debt adjustment recurrence (2.2) remains at small values (not exceeding 0.5 in magnitude) along asymptotic orbits and, hence, there are no drastic changes in D_t. Moreover, the fragility indicator f_t, computed along asymptotic orbits with $c = 0.7$, equals approximately 0.03, which corresponds to the case when firms are financed at low risk, as indicated in Sec. 2.

Now we discuss the case when the condition C1 in Proposition 4 is not satis-

fied and the related Neimark-Sacker bifurcation is degenerate. What is the result of such a bifurcation needs deeper analysis (for details see, e. g., [8, Chapter 9] and references therein). In fact, three critical values of γ are associated with three strong resonances and represent bifurcation points of codim-2. The value $\gamma = 4(1/r + 1)$ is related to strong resonance 1:2, when both the multipliers of the fixed point $\mathrm{e}^{\pm i\theta(v_{ns})} = -1$. The value $\gamma = 3(1/r + 1) =: \gamma_{1:3}$ is associated with strong resonance 1:3, when $\theta(v_{ns}) = 2\pi/3$. And for $\gamma = 2(1/r + 1) =: \gamma_{1:4}$ strong resonance 1:4 occurs, that is, $\theta(v_{ns}) = \pi/2$. In general, there may occur also 1:1 strong resonance for which $\mathrm{e}^{\pm i\theta(v_{ns})} = 1$, but this cannot happen for the fixed point F^*. Below we consider only cases of strong resonances 1:3 and 1:4, leaving the third case (1:2), which corresponds to intersection of flip and Neimark-Sacker bifurcation curves, for further studies. The dynamics of the map T in the mentioned two cases is described only numerically for the particular chosen set of parameters. For different parameter set, the general dynamical picture can be different, especially in case of strong resonance 1:4, which is much more tricky than the case 1:3.

Let us first fix $\gamma = \gamma_{1:3}$. As already visible in Fig. 2, there is no tongue related to a 3-cycle as one could expect. Fig. 6(a) shows the enlarged part of the (v, γ) parameter plane near the codim-2 bifurcation point $R_{1:3} = (v_{ns}, \gamma_{1:3})$. Though the complete picture of dynamics that can occur in the neighborhood of the point $R_{1:3}$ is unknown, certain common features can be described. For all parameter values close enough to $R_{1:3}$, the Neimark-Sacker bifurcation produces a closed invariant curve Γ surrounding the fixed point F^* and there also exists a saddle 3-cycle $\mathcal{C}_3$, which is located outside Γ and whose stable set confines its basin of attraction. In Fig. 6(b) the related part of the phase space is shown. Note that we use here the same trick as in Fig. 5(c), plotting in scale the parallelepiped area with vertices $(1133.3095, 499.9935)$, $(1133.3397, 500.0072)$, $(1133.3405, 500.0072)$, $(1133.3103, 499.9935)$. With increasing v, the curve Γ becomes larger and finally is destroyed through boundary crisis (that is, colliding with the boundary of its basin of attraction). In the (v, γ) parameter plane, the curve related to the boundary crisis of Γ touches the Neimark-Sacker bifurcation

curve at the codim-2 point $R_{1:3}$ (see Fig. 6(a)). We notice that for such a large adjustment speed γ, debt changes more sharply; however, the fragility indicator f_t computed along asymptotic orbits is still about 0.03.

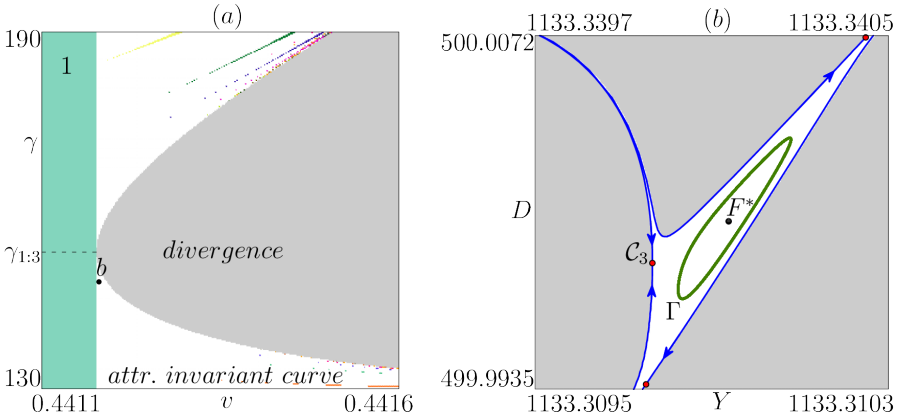

Figure 6: (Color online) (a) 2D bifurcation diagram in the (v, γ) parameter plane near the codim-2 bifurcation point $R_{1:3}$. (b) Scaled parallelepiped area (with vertices $(1133.3095, 499.9935)$, $(1133.3397, 500.0072)$, $(1133.3405, 500.0072)$, $(1133.3103, 499.9935)$) of the phase space corresponding to the point marked 'b' in (a) with $v = 0.44118$, $\gamma = 148$. Other parameters are as before.

Let us now turn to the region related to stable 4-cycle emerging from the point $R_{1:4} = (v_{ns}, \gamma_{1:4})$, at which strong resonance 1:4 occurs (see Fig. 7(a)). This case appears to be much more tricky than the strong 1:3 resonance. Detailed description of dynamics that can occur in the neighborhood of the related parameter point can be found, e. g., in [8]. Here we briefly describe the bifurcation scenario associated with the codim-2 point $R_{1:4} = (v_{ns}, \gamma_{1:4})$ for map T with the particular parameter set. As one can see in Fig. 7(a), showing a 2D bifurcation diagram in the (v, γ) parameter plane, for the values of $\gamma < \gamma_{1:4}$ being sufficiently close to $\gamma_{1:4}$, there are two regions related to multistability, $\mathcal{P}_{1\&4}$ (shown pink) and $\mathcal{P}_{\Gamma\&4}$ (shown orange). In the region $\mathcal{P}_{1\&4}$ a stable fixed point F^* coexists with a stable 4-cycle $\mathcal{C}_4^I$. The latter appears due to the fold bifurcation together with a saddle 4-cycle $\mathcal{C}_4^{II}$. In Fig. 7(b) (which corresponds to the parameter pair marked 'b' in Fig. 7(a)) we plot in scale the parallelepiped

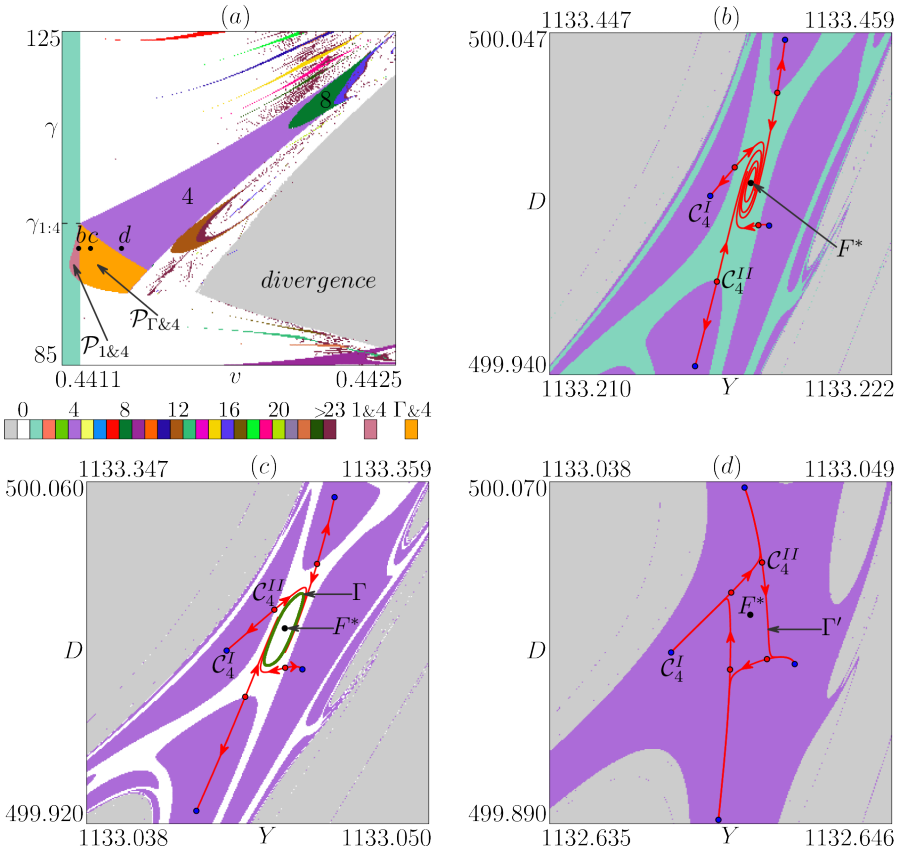

Figure 7: (Color online) (a) 2D bifurcation diagram in the (v, γ) parameter plane near the codim-2 bifurcation point $R_{1:4}$. (b)–(d) Scaled parallelepiped area with vertices (b) $(1133.21, 499.94)$, $(1133.447, 500.047)$, $(1133.459, 500.047)$, $(1133.222, 499.94)$; (c) $(1133.038, 499.92)$, $(1133.347, 500.06)$, $(1133.359, 500.06)$, $(1133.05, 499.92)$; (d) $(1132.635, 499.89)$, $(1133.038, 500.07)$, $(1133.049, 500.07)$, $(1132.646, 499.89)$ of the phase space corresponding to the respective points marked in (a) with $\gamma = 99$ and (b) $v = 0.44117$, (c) $v = 0.44122$, (d) $v = 0.44135$. Other parameters are as before.

area of the phase space with vertices $(1133.21, 499.94)$, $(1133.447, 500.047)$, $(1133.459, 500.047)$ and $(1133.222, 499.94)$, where $\mathcal{C}_4^I$ is shown by blue points, $\mathcal{C}_4^{II}$ by red points and its unstable set by red line. The stable set $W^s(\mathcal{C}_4^{II})$ (not shown explicitly in Fig. 7(b)) separates the basins of attraction of F^* (light-blue) and $\mathcal{C}_4^I$ (violet). One branch of the unstable set of $\mathcal{C}_4^{II}$ is attracted to the

node $\mathcal{C}_4^I$, while the other branch asymptotically approaches F^*.

With increasing v when a parameter point crosses Neimark-Sacker bifurcation boundary and enters the region $\mathcal{P}_{\Gamma\&4}$, the fixed point F^* becomes unstable and an invariant curve Γ appears still coexisting with the stable 4-cycle. In Fig. 7(c) (which corresponds to the parameter pair marked 'c' in Fig. 7(a)) we show scaled the parallelepiped area of the phase space with vertices $(1133.038, 499.92)$, $(1133.347, 500.06)$, $(1133.359, 500.06)$ and $(1133.05, 499.92)$, where Γ is plotted by green line. The stable set $W^s(\mathcal{C}_4^{II})$ (not explicitly shown), as before, separates the basins of two attractors.

With further increasing v, the invariant curve Γ disappears due to boundary crisis, colliding with $W^s(\mathcal{C}_4^{II})$. The cycle $\mathcal{C}_4^I$ remains the only attractor, but now both cycles are located on the closed invariant curve Γ' composed by the unstable set $W^u(\mathcal{C}_4^{II})$. In Fig. 7(d) (which corresponds to the parameter pair marked 'd' in Fig. 7(a)) there is shown the scaled parallelepiped area of the phase space with vertices $(1132.635, 499.89)$, $(1133.038, 500.07)$, $(1133.049, 500.07)$ and $(1132.646, 499.89)$, where Γ' is plotted by red line.

For the values of $\gamma > \gamma_{1:4}$, the scenario with varying v is the same as for any generic tongue. That is, with increasing v the fixed point F^* undergoes the Neimark-Sacker bifurcation and the invariant curve Γ appears around F^*. With further increasing v the cycles $\mathcal{C}_4^I$ (stable) and $\mathcal{C}_4^{II}$ (saddle) are born on Γ due to fold bifurcation. Then there follows the bifurcation sequence described above for the tongue related to period 5.

Note that if we fix v close to v_{ns} and increase γ starting from the value below $\gamma_{1:4}$ where the invariant curve Γ is the only attractor, the scenario is the following. First a pair of 4-cycles, $\mathcal{C}_4^I$ and $\mathcal{C}_4^{II}$, appear due to fold bifurcation *outside* Γ. Then Γ undergoes boundary crisis and disappears, but the unstable set $W^u(\mathcal{C}_4^{II})$ composes now a new (wider) invariant curve Γ'. Finally, $\mathcal{C}_4^I$ and $\mathcal{C}_4^{II}$ disappear due to another fold bifurcation and there remains an attracting Γ'. For a detailed description of similar scenarios of bifurcations associated with invariant curves we refer to [11] and references therein.

5. Dynamic features of business cycles

As shown above the model can describe business cycle scenarios through self-sustained oscillations taking place along stable attractors that arise as the stability condition in Proposition 2 is violated on the Neimark-Sacker bifurcation side (e. g., for increasing values of v beyond the threshold v_{ns}). The presence of such stable attractors surrounding the fixed point F^*, at least just after the bifurcation, follows from the fact that, according to Proposition 4, the mentioned bifurcation when non degenerate is of supercritical type. In this section we uncover economic mechanism for occurrence of such self-sustained oscillations and discuss the relation between dynamical complexities and the financial fragility indicator f_t defined in (2.6).

In order to highlight the economic reasons underlying the occurrence of oscillations, let us focus on the difference between the desired debt and the current debt, a term which will be denoted as δ_t in the sequel and given by

$$\delta_t = vY_t - D_t.$$

The difference δ_t influences the value of investments I_t at the same time step. Let us describe the business cycle starting from the configuration where the economy is characterized by low investment, income and debt levels. An illustrative example of such a cyclic behavior for $v = 0.47$, $\gamma = 2.4$ and the other parameters being as before is reported in Fig. 8. In this situation, sufficiently high (and positive) values of the difference δ_t contribute to investments, making them capable to support a positive demand excess. This causes, in the next step $t+1$, the rise of income which in its turn determines a further rise of investments in the subsequent steps. Further, the positiveness of δ_t determines positive debt adjustments at time $t+1$ through recurrence (2.2) and its positive trend is supported in subsequent steps due to the income increases. Along this stage of the business the variables undergo positive variations such that the difference δ_t is maintained on the positive side and investments are increasing. This occurrence is clearly distinguishable in Figs. 8(c),(d), where positive values of δ_t correspond

to increasing investments. This is in line with the usual economic interpretation according to which an increasing debt results in increasing investments, since investments come from a part of the debt use.

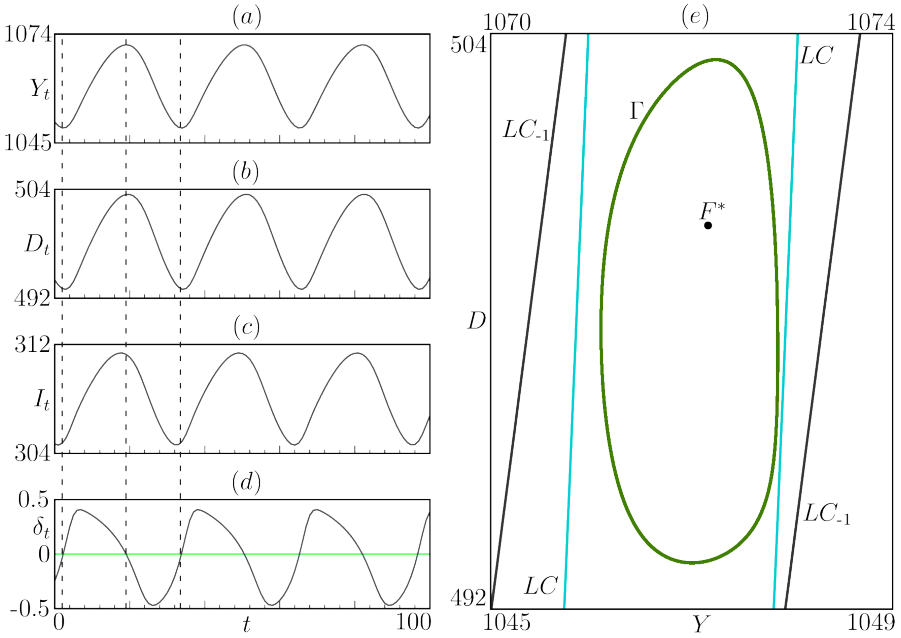

Figure 8: (Color online) (a)–(d) Time series of income (Y_t), debt (D_t), investments (I_t) and difference $\delta_t = vY_t - D_t$, respectively. (e) Scaled parallelepiped area of the phase space with vertices $(1045, 492)$, $(1070, 504)$, $(1074, 504)$, $(1049, 492)$, containing the attracting invariant curve Γ (green). The parameters are $v = 0.47, \gamma = 2.4, \alpha = 1, a_1 = 4, a_2 = 5, \bar{G} = 10, r = 0.02, c = 0.7$.

The positive variations of income and debt proceed along the time line maintaining the positiveness of δ_t until the saturation mechanism is involved. At this stage, income increments become negligible with respect to positive debt variations. Then, income contributions to investments are no more sufficient to keep them growing, thus no more compensating the negative term due to high debt levels. This causes the sign change of the difference δ_t, as well as the decrease of investments and determines negative values of the aggregate demand excess. From this stage forward the income begins to drop down together with debt.

The negative variations of the dynamic variables along the cycle maintain the negativity of δ_t and the decreasing trend of investments. Again one can see in Figs. 8(c),(d), that negative values of δ_t are paired with the decreasing trend of investments. The economic recession proceeds until the saturation mechanism is involved and income decrements become negligible with respect to the negative debt variations. At this stage, the debt level is small with respect to income and the sign of δ_t changes from the negative to the positive side, thus favoring the spread of investments. This reactivates positive variations of income and debt and the business cycle is played again.

Another example of cyclic dynamics is reported in Fig. 9, obtained with the same parameter set as in Fig. 8, except for the value of the constant factor v, which is increased from 0.47 to 0.706. In this case, the fundamental oscillatory behavior is supported by the same dynamic mechanism described above. However, now the invariant curve becomes "wavy" (see Fig. 9(e)). This means that the business cycle is perturbed by short term fluctuations due to the increased value of v (see, in particular, Figs. 9(c),(d)). To understand the nature of these deformations, one should consider the critical set of the map T and its images, as explained, for example, in [16].

Recall that the notion of critical set is typical for non-invertible maps (see [6, 15, 17–19] to cite a few). *A critical set LC* is defined as a geometric locus of points in the phase space having at least two coincident preimages. These coincident preimages are located on the set LC_{-1}, also referred to as the *set of merging preimages*. In the case of the considered map T (being continuously differentiable) LC_{-1} is the set of points (Y, D) such that[2]

$$\det DT(Y, D) = 0. \tag{5.1}$$

Equation (5.1) allows for analytical solution:

$$D = \frac{\ln s_{\pm} + \bar{G}}{\gamma + r} + \frac{\gamma v}{\gamma + r} Y, \tag{5.2}$$

[2]Note that in general LC_{-1} is only *included* in the set of points at which the determinant of the Jacobi matrix vanishes.

where

$$s_\pm = \frac{a_2}{2a_1}\left(A \pm \sqrt{A^2-4}\right), \quad A = \frac{\alpha\gamma(a_1+a_2)v(1+r)}{\gamma-1} - 2.$$

Note that (5.2) produces real values only for $\gamma > 1$ and, hence, for $\gamma \le 1$ the set $LC_{-1} = \varnothing$. The critical set is then $LC = T(LC_{-1}) = \varnothing$ for $\gamma \le 1$, while for $\gamma > 1$ it is given as

$$\left\{(\bar{Y},\bar{D}) \,:\, \bar{Y} = Y + \alpha a_2\left(\frac{a_1+a_2}{a_1 s_\pm + a_2} - 1\right), \right. \\ \left. \bar{D} = \frac{(\ln s_\pm + \bar{G})(1-\gamma)}{\gamma+r} + \frac{\gamma v(1+r)}{\gamma+r}Y\right\}_{Y\in\mathbb{R}}. \tag{5.3}$$

Clearly, (5.3) defines in the phase space two parallel lines, say, L^+ and L^-. The lines L^+ and L^- divide the phase space into three subregions, namely, two half-planes

$$\Pi^+ = \left\{(Y,D) \,:\, D > \frac{(\ln s_+ + \bar{G})(1-\gamma)}{\gamma+r} + \frac{\gamma v(1+r)}{\gamma+r}Y\right\},$$
$$\Pi^- = \left\{(Y,D) \,:\, D < \frac{(\ln s_- + \bar{G})(1-\gamma)}{\gamma+r} + \frac{\gamma v(1+r)}{\gamma+r}Y\right\},$$

each point of which has only one preimage and the band

$$B = \left\{(Y,D) \,:\, \frac{(\ln s_+ + \bar{G})(1-\gamma)}{\gamma+r} + \frac{\gamma v(1+r)}{\gamma+r}Y > D \right. \\ \left. > \frac{(\ln s_- + \bar{G})(1-\gamma)}{\gamma+r} + \frac{\gamma v(1+r)}{\gamma+r}Y\right\},$$

each point of which has three preimages. That is, map T is of type $Z_1 - Z_3 - Z_1$.

Let us turn back to comparing Figs. 8 and 9, where set of merging preimages LC_{-1} is shown with dark-gray line and the critical set LC is shown with light-blue line. For smaller value of v (in Fig. 8) the invariant curve Γ does not have any contacts/intersections neither with LC_{-1}, nor with LC. With increasing v, the curve Γ expands towards both branches of LC_{-1} and at some $v = \bar{v}$ it becomes first tangent to the lower branch of LC_{-1}. For v slightly greater than $\bar{v}$, the curve Γ has two intersections with LC_{-1} at points A_1 and A_2 (shown white in Fig. 9). As shown in [16], it then follows that Γ is tangent to LC at points $B_i = T(A_i)$, $i = 1, 2$ (shown blue in Fig. 9). When v becomes even larger,

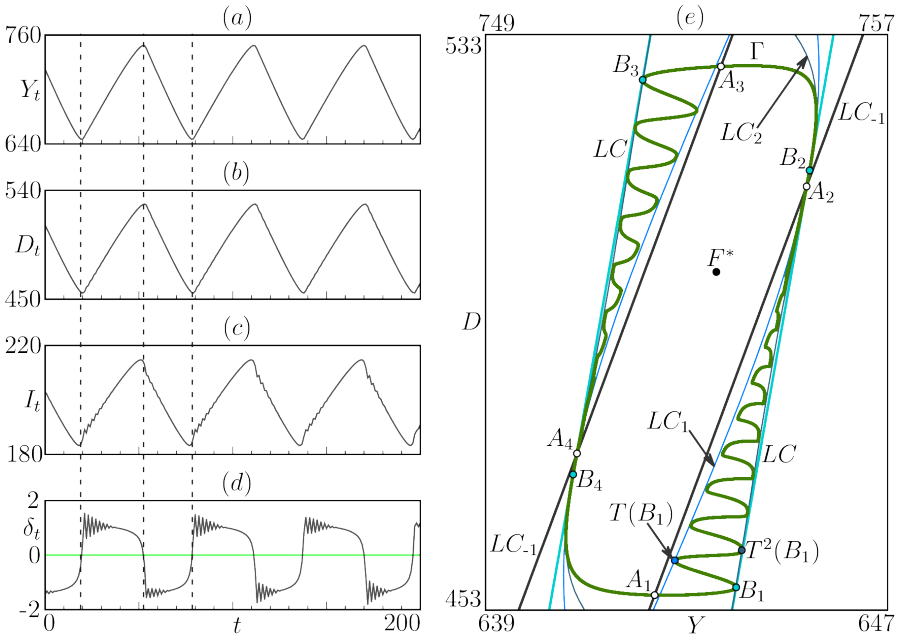

Figure 9: (Color online) (a)–(d) Time series of income (Y_t), debt (D_t), investments (I_t) and difference $\delta_t = vY_t - D_t$, respectively. (e) Scaled parallelepiped area of the phase space with vertices $(639, 453)$, $(749, 533)$, $(757, 533)$, $(647, 453)$, containing the attracting invariant curve Γ (green). The constant factor $v = 0.706$, the other parameters are as in Fig. 8.

the curve Γ expands more and another two intersections occur, now with the upper branch of LC_{-1}, at points A_3 and A_4. This produces another two points of tangency between Γ and LC, namely, $B_i = T(A_i)$, $i = 3, 4$. Consequently, Γ is also tangent to critical lines of higher rank at the successive images of B_i (see, for instance, the points $T(B_1)$ and $T^2(B_1)$ located at LC_1 and LC_2, respectively). In such a way, Γ starts to have smooth oscillations in its shape. Note that the slope of Γ at points A_i changes as v varies. It may happen that at some $v = \tilde{v}$ this slope becomes collinear to the eingenvector corresponding to zero eigenvalue[3]. After this occurrence (that is, for $v > \tilde{v}$) the curve Γ has

[3]Recall that at the points of LC_{-1} the determinant $\det DT(Y, D) = 0$ and, hence, along LC_{-1} one of the eigenvalues is always zero.

self-intersections and is not smooth any more. The interested reader can refer to [16] for more details.

Further increase of the constant factor v may lead to the rise of complex dynamics due to a homoclinic tangle and the attractor becomes a chaotic area confined by segments of critical lines of different rank. To justify this we report in Fig. 10 the maximum Lyapunov exponent $\lambda_{\max}$ computed along the orbits at increasing values of v. The simulation shows that, up to the approximate

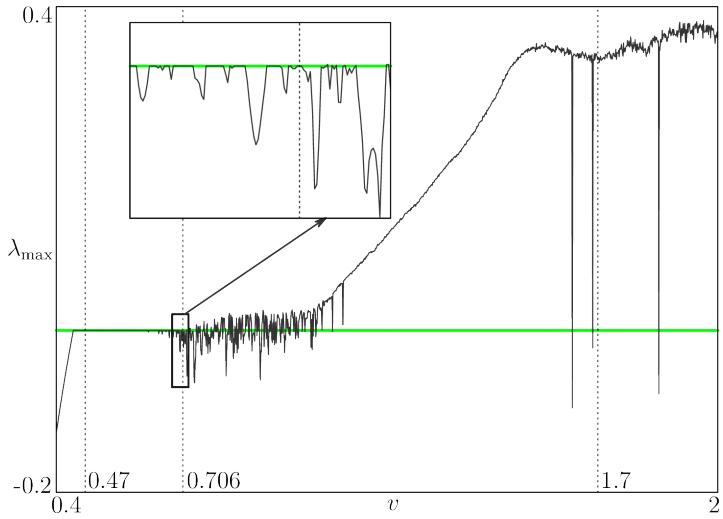

Figure 10: The maximum Lyapunov exponent versus the constant factor v. The other parameters are as in Fig. 8. The dashed lines correspond to values of v in Figs. 8, 9 and 11.

value $v \approx 0.72$, the exponent $\lambda_{\max}$ either stays at zero level or is negative. This indicates that asymptotic dynamics belongs to an attracting invariant curve or a cycle. However, when v is sufficiently high (here, approximately $v > 0.72$) $\lambda_{\max}$ is placed at positive values, except for several very small intervals where it is negative, thus attesting for the rise of chaotic behaviors.

The dynamic scenario related to the value $v = 1.7$, at which the maximum Lyapunov exponent $\lambda_{\max}$ is positive and the model is at a chaotic regime, is represented in Fig. 11. The time series (see Fig. 11(a)–(d)) show that fluctuations of economic variables no longer occur at regular intervals and the determinis-

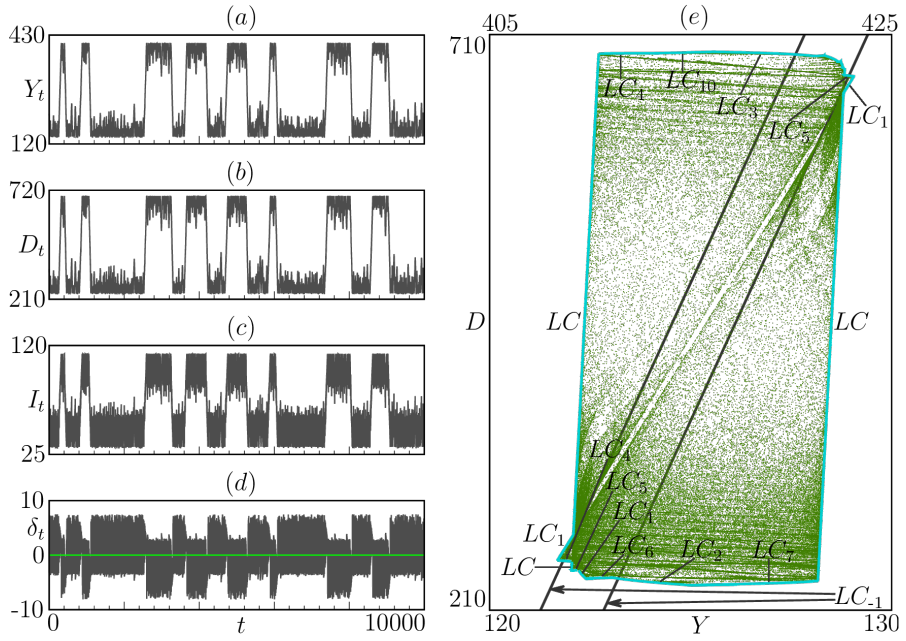

Figure 11: (Color online) (a)–(d) Time series of income (Y_t), debt (D_t), investments (I_t) and difference $\delta_t = vY_t - D_t$, respectively. (e) Scaled parallelepiped area of the phase space with vertices $(115, 210)$, $(405, 710)$, $(425, 710)$, $(135, 210)$, containing the attracting chaotic area (green). The constant factor $v = 1.7$, the other parameters are as in Fig. 8.

tic dynamics seems to be stochastically driven. We observe that, for v being large enough, income, debt and investments remain at high or low levels along extended time periods, during which short-term perturbations with lower intensities take place. In this scenario we can interpret the abrupt switching between the long term trends as a chaotic business cycle.

Finally, we point out the existing connections between the constant factor v, the financial fragility indicator f_t and the global dynamical properties of the system. Indeed, increasing values of the constant factor v determine both the increase of the dynamic complexities arising from the model and the increase of the financial fragility indicator. A first feeling of such an occurrence comes from the linear relation holding between the fragility f^* computed at the fixed

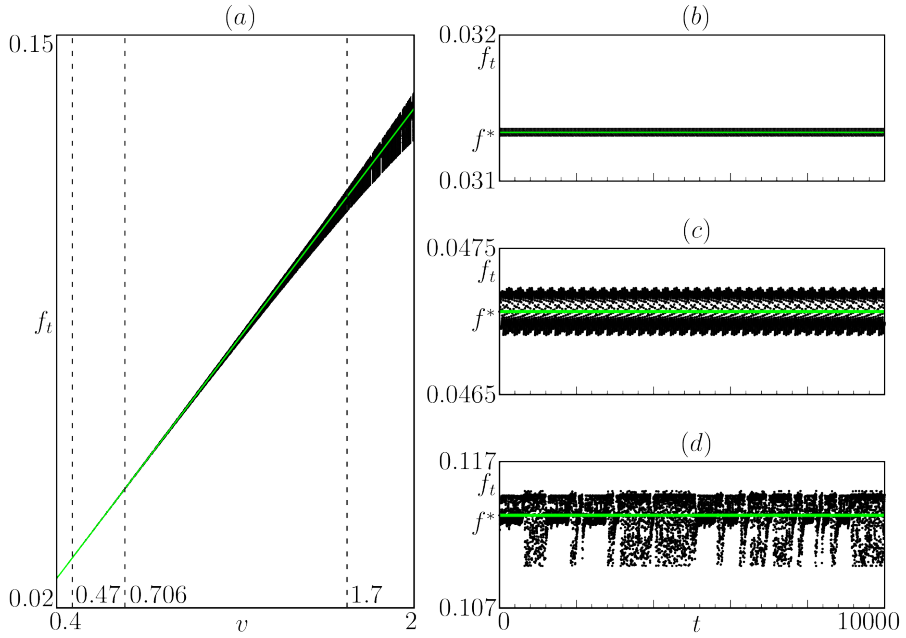

Figure 12: (a) Bifurcation diagram of financial fragility indicator f_t versus v. (b)–(d) Time series of f_t at (b) $v = 0.47$, (c) $v = 0.706$, (d) $v = 1.7$, corresponding to Figs. 8, 9 and 11 resp. The other parameters are as before.

point and the parameter v (see equation (3.2)). In Fig. 12(a), the bifurcation diagram of the financial fragility versus v is provided, thus showing that a similar relation between f_t and v is maintained, on average, also along nonstationary orbits. It is clearly visible that with larger v the value of f_t grows and its deviations from the fragility f^* (shown by green line) become more significant. The Figs. 12(b)–(d) show time series of f_t for the parameter values as in Figs. 8, 9 and 11 respectively, which attests increasing complexity of dynamics as well. Note, however, that even for larger values of v the fragility indicator is $f_t \ll 1$, which corresponds to the case of hedge finance, when the firms are financed at low risk.

6. Conclusion

We have considered a modified version of the model formulated in [5] and surveyed in [1], where a Minskyan type macroeconomic model with an endogenous debt adaptation mechanism is investigated. Our contribution is the reformulation of the above mentioned model within a discrete time framework, which is suitable for future developments that can involve expectation formation and learning processes. In addition, we have introduced a nonlinear adjustment mechanism of income to account for real world physical and social constraints. With those methodological actions, we have constructed a 2D map characterized by a nontrivial fixed point that matches the economic equilibrium.

We have studied the stability properties of the fixed point in terms of a constant factor v that describes the firms' aggregate behavior determining the desired level of debt as a certain proportion of the current income. Variations of parameter v can give rise to a flip or a Neimark-Sacker bifurcation of the fixed point. We have proved that, regardless of the other parameter values, the flip bifurcation is always subcritical, while the Neimark-Sacker bifurcation is supercritical. The structure of orbits right after the occurrence of the Neimark-Sacker bifurcation differs depending on the other parameters. In generic case, the attractor is either an invariant curve or a stable cycle of period $n, n \geq 5$, existing in a certain parameter region, often called the Arnold tongue. In both cases such asymptotic dynamics can be interpreted as a business cycle.

In addition, we have described two nongeneric cases of the Neimark-Sacker bifurcation, namely, the cases related to 1:3 and 1:4 resonances. In the former case, there is no attracting cycle of period 3, only an invariant curve. And in the parameter space instead of Arnold tongue related to period 3 one observes that the region associated with divergent orbits touches the Neimark-Sacker bifurcation curve at the codim-2 point $R_{1:3}$. It means that in the neighborhood of this parameter point, even for small deviations of v from the bifurcation value, the market becomes unstable with unbounded growth of income and debt. In the neighborhood of the other codim-2 point $R_{1:4}$, for some parameter values

one observes coexistence of a stable cycle of period 4 with either a stable fixed point or an attracting invariant curve. This implies that depending on initial condition the market may end up at two different business cycles.

As the propensity of firms to get into debt increases and the parameter v becomes distant from the Neimark-Sacker bifurcation curve, the attractor undergoes further modifications. In particular, at some level of v, the attracting invariant curve starts having "crinkles" in its form, that is the large business cycle is perturbed by short term fluctuations, thus attesting increasing complexity of dynamics. We show that this happens due to intersection of the invariant curve with the set of merging preimages. For even larger values of the bifurcation parameter, chaotic dynamics arises. Namely, the invariant curve is destroyed through a homoclinic tangle and the attractor becomes a chaotic area, which is confined by segments of critical lines of different rank.

Finally, along the line marked by the Minsky theory, the so called financial fragility indicator was considered, which provides a measure of the fragility of the financial structure of the economy. We have shown that increasing propensity of firms to get into debt is paired with increasing values of the financial fragility indicator as well as of instabilities and complexities characterizing dynamic outcomes.

Acknowledgement

We thank two anonymous referees for their useful comments and suggestions that contributed to improve the quality of this work. Usual disclaimers apply.

References

References

[1] M. Nikolaidi, E. Stockhammer, Minsky models: a structured survey, Journal of Economic Surveys 31 (5) (2017) 1304–1331 (2017).

[2] H. P. Minsky, John maynard keynes, Springer, 1976 (1976).

[3] H. P. Minsky, Inflation, recession and economic policy, Brighton, Sussex: Wheatsheaf Books, 1982 (1982).

[4] H. P. Minsky, H. Kaufman, Stabilizing an unstable economy, Vol. 1, McGraw-Hill New York, 2008 (2008).

[5] R. C. Jump, J. Michell, E. Stockhammer, A strategy switching approach to minskyan business cycles (slides), http://www.postkeynesian.net/downloads/events/Jump_et_al_2017_V4vDeWI.pdf (2017).

[6] I. Gumowski, C. Mira, Dynamique chaotique: transformations ponctuelles, transition, ordre-désordre, Cepadues, 1980 (1980).

[7] R. Devaney, An introduction to chaotic dynamical systems, Westview press, 2008 (2008).

[8] Y. A. Kuznetsov, Elements of applied bifurcation theory, Vol. 112, Springer Science & Business Media, 2013 (2013).

[9] P. L. Boyland, Bifurcations of circle maps: Arnol'd tongues, bistability and rotation intervals, Communications in Mathematical Physics 106 (3) (1986) 353–381 (1986).

[10] I. Sushko, T. Puu, L. Gardini, The hicksian floor–roof model for two regions linked by interregional trade, Chaos, Solitons & Fractals 18 (3) (2003) 593–612 (2003).

[11] A. Agliari, G.-I. Bischi, R. Dieci, L. Gardini, Global bifurcations of closed invariant curves in two-dimensional maps: a computer assisted study, International Journal of Bifurcation and Chaos 15 (04) (2005) 1285–1328 (2005).

[12] N. Leonov, Map of the line onto itself, Radiofisica 3 (3) (1959) 942–956 (1959).

[13] J. P. Keener, Chaotic behavior in piecewise continuous difference equations, Transactions of the American Mathematical Society 261 (2) (1980) 589–604 (1980).

[14] L. Gardini, F. Tramontana, Border collision bifurcation curves and their classification in a family of 1d discontinuous maps, Chaos, Solitons & Fractals 44 (4-5) (2011) 248–259 (2011).

[15] C. Mira, L. Gardini, A. Barugola, J.-C. Cathala, Chaotic dynamics in two-dimensional noninvertible maps, Vol. 20, World Scientific, 1996 (1996).

[16] C. E. Frouzakis, L. Gardini, I. G. Kevrekidis, G. Millerioux, C. Mira, On some properties of invariant sets of two-dimensional noninvertible maps, International Journal of Bifurcation and Chaos 7 (06) (1997) 1167–1194 (1997).

[17] R. Abraham, C. Mira, L. Gardini, Chaos in discrete dynamical systems: A visual introduction in 2 dimensions, Springer, 1997 (1997).

[18] A. Agliari, G.-I. Bischi, L. Gardini, Some methods for the global analysis of dynamic games represented by iterated noninvertible maps, in: Oligopoly dynamics, Springer, 2002, pp. 31–83 (2002).

[19] G. I. Bischi, F. Lamantia, D. Radi, Qualitative methods in continuous and discrete dynamical systems, in: Qualitative Theory of Dynamical Systems, Tools and Applications for Economic Modelling, Springer, 2016, pp. 1–159 (2016).

Appendix A. Proof of Proposition 3

The proof is merely technical and uses the well-known projection method for center manifold computation, described in detail in [8]. Therefore only a sketch is provided.

We decompose the map $\widetilde{T}$ into Taylor series in the neighborhood of the fixed point $(0,0)$:

$$\widetilde{T}(x) = \widetilde{J}x + F(x) = \widetilde{J}x + \frac{1}{2}B(x,x) + \frac{1}{6}C(x,x,x) + O(\|x\|^4), \qquad \text{(A.1)}$$

where[4] $x = (Y, D)^{\mathrm{T}}$, $\widetilde{J}$ is the Jacobian matrix of $\widetilde{T}$ evaluated at $(0,0)$ and

$$B_i(x,y) = \sum_{j,k=1}^{2} \frac{\partial^2 \widetilde{T}_i(0,0)}{\partial\xi_j \partial\xi_k} x_j y_k, \quad C_i(x,y,u) = \sum_{j,k,l=1}^{2} \frac{\partial^3 \widetilde{T}_i(0,0)}{\partial\xi_j \partial\xi_k \partial\xi_l} x_j y_k u_l, \quad i = 1,2.$$

Clearly $B_2(x,y) \equiv 0$ and $C_2(x,y,u) \equiv 0$. Let us denote as q the eigenvector of $\widetilde{J}$ corresponding to the eigenvalue $\mu = -1$. We also compute the adjoint eigenvector p such that $\widetilde{J}^{\mathrm{T}} p = \mu p$ and $\langle p, q\rangle = 1$.[5] Then the center manifold W_{v_f} of $\widetilde{T}_{v_f}$ is represented by a function whose Taylor series starts from quadratic terms and the restriction $\widetilde{T}_{v_f}|_{W_{v_f}}$ takes the form

$$u \mapsto -u + a(0)u^2 + b(0)u^3 + O(u^4), \qquad \text{(A.2)}$$

where the expressions for coefficients $a(0)$ and $b(0)$ include $\widetilde{J}$, q, p, $B(q,q)$ and $C(q,q,q)$. By the Theorem about the normal form for the flip bifurcation (see, [8, p. 121]), the map (A.2) is topologically conjugate to

$$\xi \mapsto -\xi + c(0)\xi^3 + O(\xi^4),$$

where

$$c(0) = a^2(0) + b(0) = \frac{1}{6}\langle p, C(q,q,q)\rangle - \frac{1}{2}\langle p, B(q, (\widetilde{J} - \mathrm{Id})^{-1} B(q,q))\rangle$$

with Id being the identity matrix. Direct computation gives $c(0)$ in the form (4.3).

Appendix B. Proof of Proposition 4

Again the proof is simply technical and based on the known method described in [8]. Hence, only a sketch is provided.

[4] Here the upper index $^{\mathrm{T}}$ denotes the transpose operator

[5] The function $\langle\cdot,\cdot\rangle$ denotes the scalar product.

We again decompose the map $\widetilde{T}$ into Taylor series (A.1) in the neighborhood of $(0,0)$. For $v = v_{ns}$ the Jacobian matrix $\widetilde{J}$ has two complex conjugate eigenvalues $\mu = \mathrm{e}^{i\theta_0}$ and $\bar{\mu} = \mathrm{e}^{-i\theta_0}$, $\theta_0 = \theta(v_{ns})$, located at the unit circle. Let us denote as q the eigenvector of $\widetilde{J}$ related to μ, then $\bar{q}$ corresponds to $\bar{\mu}$. Let p be the adjoint eigenvector such that $\widetilde{J}^{\mathrm{T}} p = \bar{\mu} p$ and $\langle p, q\rangle = 1$.[6] Any real-valued vector $x = (Y, D)^{\mathrm{T}}$ can be represented as $x = zq + \bar{z}\bar{q}$ for some complex z. The new complex variable is then defined by $z = \langle p, x\rangle$ and the map $\widetilde{T}$ in terms of this new variable becomes

$$z \mapsto \mu z + g(z, \bar{z}, p), \quad g(z, \bar{z}, p) = \langle p, F(zq + \bar{z}\bar{q})\rangle. \tag{B.1}$$

The Taylor series of the function g with respect to $(z, \bar{z})$ starts with quadratic terms and has coefficients denoted g_{kl}, $k + l \geq 2$. Taking into account the decomposition of $F(\cdot)$ into sum of $B(\cdot,\cdot)$, $C(\cdot,\cdot,\cdot)$ and higher order terms (see (A.1)), the coefficients g_{kl} with $k + l \leq 3$ are computed as scalar products of p and functions B and C over arguments q, $\bar{q}$. Omitting further technical details, we recall that by an invertible smooth change of complex coordinate map (B.1) can be transformed into (4.4).

Note that to have the suitable transformation, the non-degeneracy conditions (i) $r'(v_{ns}) \neq 0$ and (ii) $\mathrm{e}^{ik\theta_0} \neq 1$, $k = 1, 2, 3, 4$ are required. By straightforward computation we get that

$$r(v) = \sqrt{\frac{\alpha a_1 a_2 \gamma v(1 + r)}{a_1 + a_2} + 1 - \gamma},$$

from which the condition (i) follows. As for the condition (ii), it is always true for $k = 1$, while the values $k = 2, 3, 4$ imply the restriction C1.

[6] Recall that for complex valued vectors the scalar product is defined as $\langle p, q\rangle = \bar{p}_1 q_1 + \bar{p}_2 q_2$.